Influence of the promoter in Pd behaviour in Three-way Catalysts upon dynamic, cycling CO/NO conditions: a structural and chemical approach

Anna Kubacka,[1] Ana Iglesias-Juez,[1] Marco Di Michiel,[2] Mark A. Newton,[2,*] Marcos Fernández-García,[1,*]

[1] Instituto de Catálisis y Petroleoquímica, CSIC, C/Marie Curie 2, 28049, Madrid, Spain.
[2]European Synchrotron Radiation Facility, 6, Rue Jules Horowitz, BP-220, Grenoble, France.

Notes on EXAFS Data Analysis

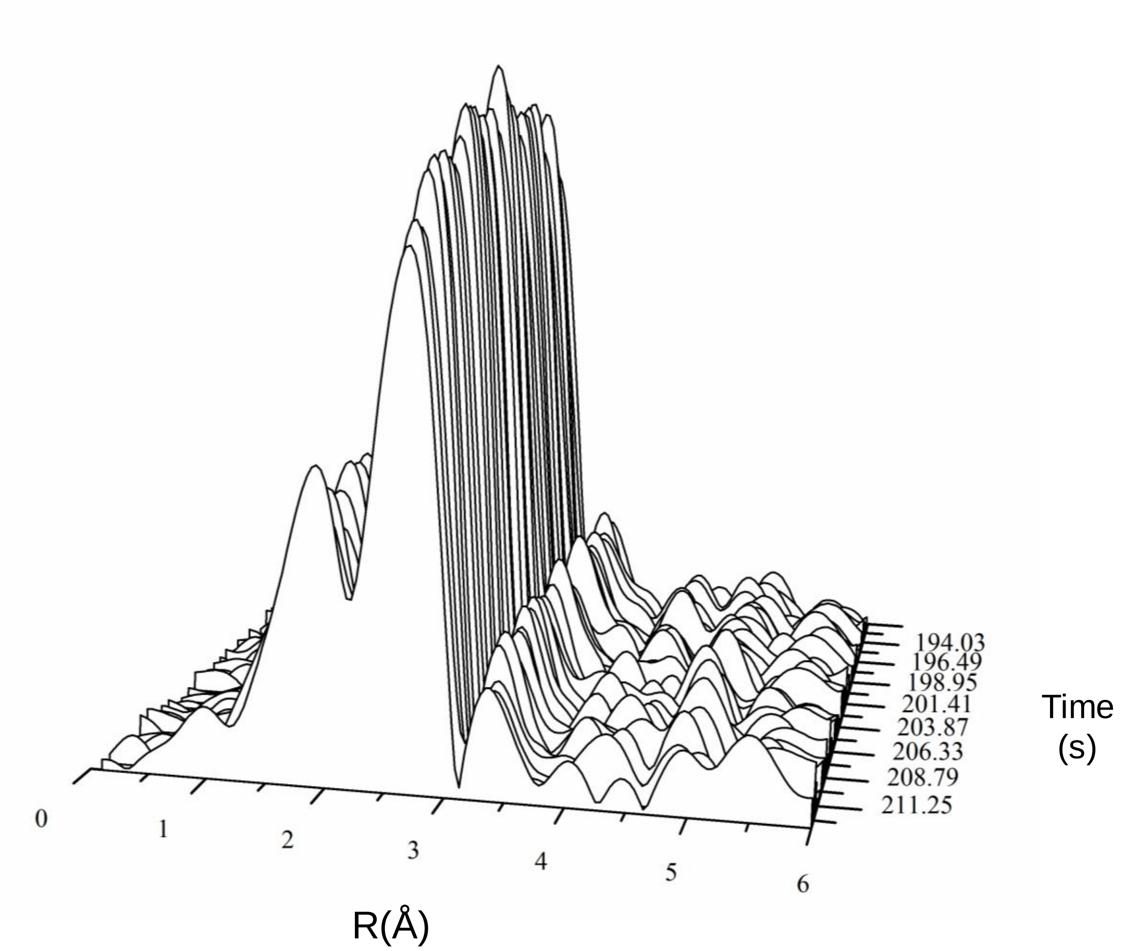

Fig. S1. Fourier Transform of 4Pd3ZCA EXAFS data taken during a CO step of a CO/NO cycling treatment at 673 K. Total temporal span 13.86 s.

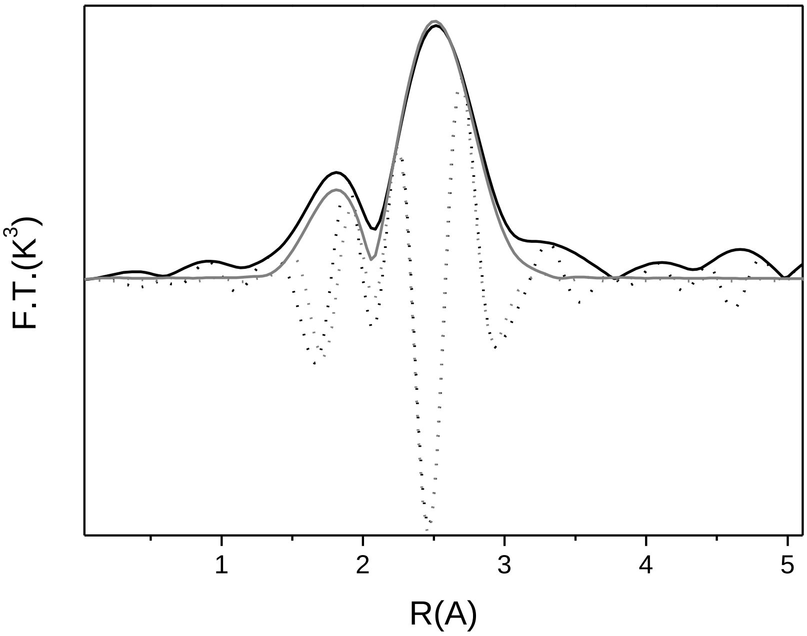

Fig. S2. FT and imaginary part of the EXAFS spectrum taken at the end part (13 s) of the CO step (Fig. S1). Fitting results are also presented (gray line).

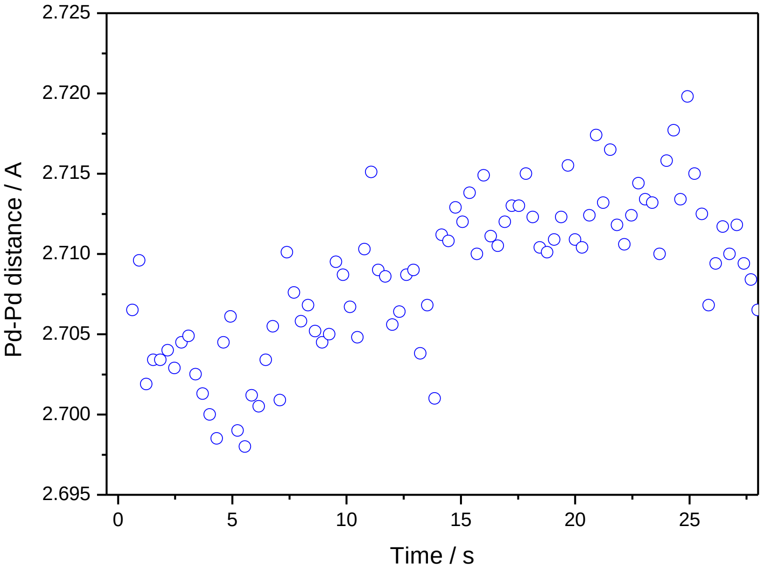

Fig. S3. Pd-Pd 1st shell EXAFS distance for the 4Pd3ZCA catalyst over a CO/NO cycling treatment at 673 K. Total temporal span 2 x 13.86 s.

The Fourier Transform´s of EXAFS signal indicates morphological changes of the metal particles during the CO/NO treatment (Fig. S1), which were subjected to fitting using exclusively a Pd-Pd single shell as detailed in the experimental section. The fitting outcome is exemplified in Fig. S2. The low-R region, below 3.0 A, is essentially described by the Pd-Pd first shell throughout the cycling treatment. The inclusion of an additional Pd-C shell in the fitting drive to unphysical results in the C.N. and distance of such contribution. This indicates that distinctive information about the PdCx phase (C atom backscatterer) is essentially loss in the EXAFS FTs current analysis although it is (indirectly) reflected in the mild intensity variation of the main FT peak (see main paper for a full discussion). Corresponding Pd-Pd C.N.s (Fig. 2 main paper) and distances (Fig. S3) of the first Pd-Pd shell quantify the changes mentioned and presented by the metal under reaction conditions.

Concerning the EXAFS analysis results just described a word of caution can be raised as the use of an harmonic (standard) approximation for describing the local structure of the solid is challenged by its nanostructured nature (e.g. mainly although not exclusively surface contribution as for EXAFS) as well as for inharmonic vibrational contributions derived of our measurement temperature. Both effects are not considered in the standard fitting EXAFS procedure. We particularly note that C.N. is typically underestimated within the standard approach while the distance must need to be corrected, typically using experimental procedures including comparison with spectra taken at low temperature.

Concerning the analysis of the 4Pd3ZCA sample, we emphasize the fact that 1st Pd-Pd shell C.N.s presented variation between two limiting values of ca. 7.2 and 7.7, with a standard error of ca. 10 % (Fig. 2 of the main paper). While this means that we can not give quantitative information about the morphological modification of Pd particle morphology, the (ascending or descending vs. time) trends presented in Fig. 2 have been consistently obtained for Pd-based TWCs materials (see .refs. 18, 24 of the main paper) and are thus representative of the noble metal particle behavior. Note however that only through the combined application of the three techniques presented, XAS, XRD and DRIFTS, the study was able to produce a complete picture of the metal nanoparticles morphological evolution during reaction. Details of the corresponding analysis are described in the main text of the article.

Also, we note that the above mentioned EXAFS fitting procedures can put Pd-Pd XRD and EXAFS derived distance observables in common basis (see full discussion at ref. 24 of the main paper). Here we only stress the fact that both techniques reported roughly similar, featureless trends (Figs. 4 and S3) for 4Pd3ZCA but that XRD results are significantly more robust in terms of error and significance (e.g. less affected by fitting assumptions in this specific case).